Deforestation in Amazonia impacts riverine carbon dynamics

F. Langerwisch[1,2], A. Walz[3], A. Rammig[1,4], B. Tietjen[5,2], K. Thonicke[1,2], W. Cramer[6]

[1] Earth System Analysis, Potsdam Institute for Climate Impact Research (PIK), P.O. Box 60 12 03, Telegraphenberg A62, D-14412 Potsdam, Germany
[2] Berlin-Brandenburg Institute of Advanced Biodiversity Research (BBIB), 14195 Berlin, Germany
[3] Institute of Earth and Environmental Science, University of Potsdam, Karl-Liebknecht-Str. 24-25, D-14476 Potsdam-Golm, Germany
[4]TUM School of Life Sciences Weihenstephan, Land Surface-Atmosphere Interactions, Technische Universität München, Hans-Carl-von-Carlowitz-Platz 2, 85354 Freising, Germany
[5] Biodiversity and Ecological Modelling, Institute of Biology, Freie Universität Berlin, Altensteinstr. 6, D-14195 Berlin, Germany
[6] Institut Méditerranéen de Biodiversité et d'Ecologie marine et continentale (IMBE), Aix Marseille Université, CNRS, IRD, Avignon Université, Technopôle Arbois-Méditerranée, Bât. Villemin - BP 80, F-13545 Aix-en-Provence cedex 04, France

Correspondence to: F. Langerwisch (langerwisch@pik-potsdam.de)

Abstract

Fluxes of organic and inorganic carbon within the Amazon basin are considerably controlled by annual flooding, which triggers the export of terrigenous organic material to the river and ultimately to the Atlantic Ocean. The amount of carbon imported to the river and the further conversion, transport and export of it depend on temperature, atmospheric CO_2, terrestrial productivity and carbon storage, as well as discharge. Both, terrestrial productivity and discharge, are influenced by climate and land use change. The coupled LPJmL and RivCM model system (Langerwisch et al., 2015) has been applied to assess the combined impacts of climate and land-use change on the Amazon riverine carbon dynamics. Vegetation dynamics (in LPJmL) as well as export and conversion of terrigenous carbon to and within the river (RivCM) are included. The model system has been applied for the years 1901 to 2099 under two deforestation scenarios and with climate forcing of three SRES emission scenarios, each for five climate models. We find that high deforestation (BAU scenario) will strongly decrease (locally by up to 90%) riverine particulate and dissolved organic carbon amount until the end of the current century. At the same time, discharge increases leave net carbon transport during the first decades of the century roughly unchanged only if a sufficient area is still forested. After 2050 the amount of transported carbon will decrease drastically. In contrast to that, increased temperature and atmospheric CO_2 concentration determine the amount of riverine inorganic carbon stored in the Amazon basin. Higher atmospheric CO_2 concentrations increase riverine inorganic carbon amount by up to 20% (SRES A2). The changes in riverine carbon fluxes have direct effects on carbon export, either to the atmosphere via outgassing, or to the Atlantic Ocean via discharge. The outgassed carbon will increase slightly in the Amazon basin, but can be regionally reduced by up to 60% due to deforestation. The discharge of organic carbon to the ocean will be reduced by about 40% under the most severe deforestation and climate change scenario. These changes would have local and regional consequences on the carbon balance and habitat characteristics in the Amazon basin itself but also in the adjacent Atlantic Ocean.

1 Introduction

The Amazon basin, defined as the drainage area of the Amazon River, covers approximately six million square kilometres, and more than 70% of it is still covered with intact rainforest (Nobre, 2014). The amount of carbon in biomass in Amazonian rainforest is estimated to be $93 \pm 23 \times 10^{15}$ g C (Malhi et al., 2006). This biomass is stored in a wide range of diverse habitats, including tropical rainforest and savannahs, as well as numerous aquatic habitats, like lakes and wetlands (Goulding et al., 2003; Eva et al., 2004; Keller et al., 2009; Junk, 1997). The large diversity in habitats, partly already founded in the geologic formation of Amazonia, leads to a high diversity of animal and plant species (Hoorn et al., 2010), making the Amazon rainforest one of Earth's greatest collections of biodiversity. The Amazon River,

which floods annually large parts of the forest, plays an important role in supporting the diversity of Amazonian ecosystems. The flooding is most decisive for the coupling of terrestrial and aquatic processes by transporting organic material from the terrestrial ecosystems to the river (Hedges et al., 2000). The input of terrigenous organic material (Melack and Forsberg, 2001; Waterloo et al., 2006), acts, for instance, as fertilizer and food source (Anderson et al., 2011; Horn et al., 2011), and is a modifier of habitats and interacting local carbon cycles (Hedges et al., 2000; Irmler, 1982; Johnson et al., 2006; McClain and Elsenbeer, 2001). Across the Amazon basin, the amount of carbon released from the river into the atmosphere and exported to the ocean are the two most important processes when assessing the effects riverine carbon dynamics under climate change. Approximately 470×10^{12} g C yr^{-1} is exported to the atmosphere as CO_2 (Richey et al., 2002), in comparison with about 32.7×10^{12} g C yr^{-1} of total organic carbon (TOC) is exported to the Atlantic Ocean (Moreira-Turcq et al., 2003). It is estimated that the large scale outgassing of carbon from the Amazon River plays an important role in assessing the future carbon balance of the Amazon basin, integrating riverine as well as terrestrial processes.

Deforestation continues to be the largest threat to Amazonia. The transformation of tropical rainforest to cropland and pasture impacts ecosystem stability profoundly due to altered climate regulation and species richness (Foley et al., 2007; Lawrence and Vandecar, 2014; Malhi et al., 2008; Spracklen et al., 2012). Until the year 2012 approximately 20% of the original forest of the Brazilian part of the Amazon basin has been deforested, corresponding to an area of about 750,000 km^2 (Godar et al., 2014; INPE, 2013). This deforestation was mainly driven by the land expansion for soybean and cattle production and the expansion of the road network (Malhi et al., 2008; Soares-Filho et al., 2006). Governmental and conservation efforts have helped to decrease recent deforestation rates (Nepstad et al., 2014) but economic instability might reverse this trend (Aguiar et al., 2016; Fearnside, 2015). Together with climate change effects and forest burning, land cover change is predicted to release carbon at rates of $0.5\text{-}1.0\times10^{15}$ g C yr^{-1} from this area (Potter et al., 2009). Additionally, the annual CO_2 efflux from pasture soils exceeds that of mature and secondary forest (Salimon et al., 2004). Furthermore, the effects of deforestation on terrestrial carbon storage and fluxes persist several decades after logging because the forest needs about 25 years to recover approximately 70% of its original biomass, and at least another 50 years for the remaining 30% after abandonment of agriculture (Houghton et al., 2000; Poorter et al., 2016).

Deforestation immediately reduces the terrestrial organic carbon pools, which fuel riverine respiration (Mayorga et al., 2005), while increasing the velocity and amount of runoff, as well as the discharge (Foley et al., 2002; Costa et al., 2003). Additionally, climate change alters precipitation which then affects inundation patterns (Langerwisch et al., 2013), such as temporal shifts in high and low water months and changes of inundated area. The combined effects of deforestation and climate change have the potential to tremendously alter the exported terrigenous carbon fluxes, the amount of carbon emitted to the atmosphere and exported the ocean. The local export of terrestrial organic carbon to the river changes the nutrient supply and therefore alters the habitat for riverine plants and animals, (Hamilton, 2010).

The aim of our study is to elaborate on these combined effects of climate change and deforestation on the riverine carbon fluxes, on the export of organic material into the Atlantic Ocean and on the outgassing of riverine carbon to the atmosphere. By considering the interactions between riverine and terrestrial carbon processes a complete view on future changes in the regional and basin-wide carbon balance can be achieved for the Amazon basin.

To address these issues basin-wide data are needed, which not only describe the current situation but also assess future changes, expanding our knowledge obtained from on-site measurements. To partly overcome these limitations we make use of the well-established dynamic global vegetation model LPJmL together with the riverine carbon model RivCM. While LPJmL (Bondeau et al., 2007; Gerten et al., 2004; Rost et al., 2008; Sitch et al., 2003) provides plausible estimates for the carbon and water pools and fluxes within the coupled soil-vegetation system, RivCM (Langerwisch et al., 2015) focuses on the export, conversion and transport of terrestrial fixed carbon in the river and to the atmosphere and ocean. In Langerwisch et al. (2015) the solely effects of climate change have been estimated. The results of the mentioned study show that climate change causes a doubling of riverine organic carbon in the Southern and Western basin while reducing it by 20% in the eastern and northern parts towards the end of this century. In contrast, the amount of riverine inorganic carbon shows a 2- to 3-fold increase in the entire basin, independent of the climate change scenario (SRES). The export of carbon to the atmosphere increases on average by about 30%. The amount of organic carbon exported to the Atlantic Ocean depends on the SRES scenario and is projected to either decrease by about 8.9% (SRES A1B) or increase by about 9.1% (SRES A2). The current study, which is an extension of Langerwisch et al. (2015) goes one step further and investigates the combined effects of climate change and deforestation on the riverine carbon dynamics. The coupled model LPJmL-RivCM was forced by several climate change and deforestation scenarios that cover a wide range of uncertainties. We estimated temporal and spatial changes in three riverine carbon pools as well as changes in carbon emissions to the atmosphere and carbon export the ocean.

2 Methods

To assess the impacts of climate change and deforestation on riverine carbon pools and fluxes in the Amazonian watershed we applied the model system of LPJmL and RivCM. RivCM is a grid-based model that assesses the transport and export of carbon at monthly time steps and is driven climate data and terrestrial carbon pools (Langerwisch et al., 2015). Climate inputs are taken from different global climate model simulations driven by three SRES scenarios (A1B, A2 and B1; Nakićenović et al., 2000). Terrestrial carbon inputs are calculated by the process-based dynamic global vegetation and hydrology model LPJmL (Bondeau et al., 2007; Gerten et al., 2004; Rost et al., 2008; Sitch et al., 2003). To estimate soil and vegetation carbon, LPJmL uses the above mentioned climate data and a set of deforestation scenarios from a regional projections by SimAmazonia (Soares-Filho et al., 2006). An overview of the interconnection between the two models and the scenarios is given in Figure 1.

2.1 Model descriptions

2.1.1 LPJmL – a dynamic global vegetation and hydrology model

The process-based global vegetation and hydrology model LPJmL (Bondeau et al., 2007; Gerten et al., 2004; Rost et al., 2008; Sitch et al., 2003) simulates the dynamics of potential natural vegetation and thus carbon pools for vegetation, litter and soil and corresponding water fluxes, in daily time steps and on a spatial resolution of 0.5 × 0.5 degree (lat/lon). The main processes included are photosynthesis (modelled according to Collatz et al., 1992; Farquhar et al., 1980), auto- and heterotrophic respiration, establishment, mortality, and phenology. For calculating these main processes LPJmL uses climate data (temperature, precipitation, and cloud cover), atmospheric CO_2 concentration, and soil type as input The simulated water fluxes include evaporation, soil moisture, snowmelt, runoff, discharge, interception, and transpiration, which are directly linked to abiotic and biotic properties. In each grid cell LPJmL calculates the performance of nine plant functional types, which represent an assortment of species classified as being functionally similar. In the Amazon basin primarily three of these types are present, namely tropical evergreen and deciduous trees and C4 grasses. In addition to the potential natural vegetation LPJmL can simulate the dynamics of 16 user-defined crops and pasture on area that is not covered by natural vegetation. In analogy to natural vegetation, LPJmL evaluates carbon storage in vegetation, litter and soil as well as water fluxes for these areas.

LPJmL has been shown to reproduce current patterns of biomass production (Cramer et al., 2001; Sitch et al., 2003), carbon emission through fire (Thonicke et al., 2010), also including managed land (Bondeau et al., 2007; Fader et al., 2010; Rost et al., 2008), and water dynamics (Biemans et al., 2009; Gerten et al., 2004, 2008; Gordon et al., 2004; Wagner et al., 2003). The simulated patterns in water fluxes, like evapotranspiration, runoff and soil moisture, are comparable to stand-alone global hydrological models (Biemans et al., 2009; Gerten et al., 2004; Wagner et al., 2003).

2.1.2 RivCM – a riverine carbon model

RivCM is a process-based model that calculates four major ecological processes related to the carbon budget of the Amazon River (Figure 1B). These processes include (1) mobilization, (2) decomposition and (3) respiration within the river, and (4) outgassing of CO_2 to the atmosphere (Langerwisch et al., 2015). During mobilization parts of terrigenous litter and soil carbon, as it is provided by LPJmL, is imported to the river, depending on inundated area. The further processing of the terrigenous carbon in the river happens during its decomposition, which represents the manual breakup, and its respiration, representing the biochemical breakup. Finally the CO_2 that is produced during respiration can outgas if the saturation concentration is exceeded (Langerwisch et al., 2015). These four processes directly control the most relevant riverine carbon pools, namely particulate organic carbon (POC), dissolved organic carbon (DOC), and inorganic carbon (IC), as well as outgassed atmospheric carbon (representing CO_2), and exported riverine carbon to the ocean (either as POC, DOC, or IC).

The model is coupled to LPJmL by using the calculated monthly litter and soil carbon and water amounts as inputs. It operates at the spatial resolution of 0.5 × 0.5 degree (lat/lon) and on monthly time steps. The ability of the coupled model LPJmL-RivCM to reproduce current conditions in riverine carbon concentration and export to either the atmosphere or the ocean has been shown and discussed by Langerwisch et al. (2015). A validation of the carbon pools and fluxes with observed data shows that RivCM produces results that are within the range of observed concentrations of both organic and inorganic carbon pools, but it underestimates the outgassed carbon strongly while it overestimates the carbon discharged to the ocean. Nevertheless we are certain that relative changes in the carbon can be assessed by the model. Here, we therefore utilize the coupled model system of LPJmL and RivCM to assess the combined impacts of climate change and deforestation.

2.2 Model simulation

All transient LPJmL runs were preceded by a 1000-year spin-up during which the pre-industrial CO_2 level of 280 ppm and the climate of the years 1901-1930 have been repeated to obtain equilibria for vegetation, carbon, and water pools. All transient runs of the coupled model LPJmL-RivCM have been preceded by a 90-years-spinup during which the climate and CO_2 levels of 1901-1930 have been repeated to obtain equilibria for riverine carbon pools.

LPJmL-RivCM was run on a 0.5° × 0.5° degree (lat/lon) spatial resolution for the years 1901 to 2099. For the estimation of the impact of projected climate change (CC) and deforestation (Defor), simulations have been conducted driven by five General Circulation Models (GCMs), each calculated for three SRES emission scenarios, and three LUC scenarios.

2.2.1 Climate change and deforestation data sets

To assess the effect of future climate change, projections of five GCMs (see also Jupp et al., 2010; Randall et al., 2007), using three SRES scenarios (A1B, A2, B1) (Nakićenović et al., 2000) have been applied (Figure 1A). The GCMs, namely MIUB-ECHO-G, MPI-ECHAM5, MRI-CGCM2.3.2a, NCAR-CCSM3.0, UKMO-HadCM3, cover a wide range in terms of temperature and precipitation and have therefore been chosen to account for uncertainty in climate projections. The emission scenario SRES A1B describes a development of very rapid economic growth with convergence among regions, and a balanced future energy source between fossil and non-fossil. SRES A2 describes a development of a very heterogeneous world with slow economic growth. And SRES B1 describes a development of converging world similar to A1B but with more emphasis on service and information economy.

To estimate the additional effects of deforestation on riverine carbon pools and fluxes three land use scenarios were applied: two scenarios directly relate to different intensity of deforestation, and one represents a reference scenario with complete coverage by natural vegetation (NatVeg scenario, hereafter). The two deforestation scenarios are based on the SimAmazonia projections (Soares-Filho et al., 2006, see also Figure S1). The authors estimate the development of deforestation in the Amazon basin until 2050 based on historical trends and projected developments. In the business-as-usual scenario (BAU) they assume that recent deforestation trends continue, the number of paved highways increases, and new protected

areas are not established. In contrast, deforestation is more efficiently controlled in the governance scenario (GOV). For this scenario the authors assume that the Brazilian environmental legislation is implemented across the Amazon basin and the size of the area under the *Protected Areas Program* increases. The SimAmazonia scenarios cover the years from 2001 to 2050. The period between 2051 and 2099 was included into our study to show the long term effects of deforestation, while further deforestation is neglected over this period. In addition deforestation rates preceding the deforestation scenarios were derived from extrapolating the data into the past. LPJmL requires historic land-cover information to correctly capture transient carbon dynamics. The model starts to simulate vegetation dynamics from bare ground and can't be initialized with a land-cover map of a particulate year. It was therefore necessary to develop an approach which produced consistent land-cover information for the (undisturbed) past and the deforestation scenarios. For that, the mean annual rate of deforestation was calculated for the reference period of 2001 to 2005 (Eq. (1)) and this rate was applied to calculate the fraction of deforested area F_t for the years 1901 to 2000 for each cell (Eq. (2)).

$$r = \left(\sum_{t=2001}^{2005} \frac{F_t}{F_{t+1}} \right) \times \frac{1}{2006 - 2001} \quad (1)$$

$$F_t = F_{2001} \times r^{2001-t} \quad (2)$$

To evaluated spatial differences in the basin we defined three sub-regions (see Table 1). Three regions were selected for further detailed analysis and differ in projected changes in inundation patterns and in deforestation intensity. R1 is located in the Western basin with projected increase in inundation length and inundated area (Langerwisch et al., 2013) combined with low land use intensity. R2 is a region covering the Amazon main stem with intermediate changes in inundation (Langerwisch et al., 2013) and intermediate land use intensity. And R3 is a region with projected decrease in duration of inundation and inundated area (Langerwisch et al., 2013) combined with high land use intensity. In the deforestation scenarios we assume that on 15% of the deforested area soy bean is grown and 85% of the area is used as pasture for beef production (Costa et al., 2007).

2.3 Analysis of simulation results

The separate effect of deforestation (E_{Defor}) is estimated by calculating the differences between future carbon amounts (2070-2099) produced in the deforestation scenarios (GOV or BAU) and future carbon amounts produced in the potential natural vegetation scenario (NatVeg), where no deforestation is assumed. The combined effect of climate change and deforestation ($E_{CCDefor}$) is estimated by calculating the differences between future carbon amounts produced in the deforestation scenarios and reference carbon amounts (1971-2000) produced in the NatVeg scenario. We analysed all four riverine carbon pools (riverine particulate organic carbon (POC), dissolved organic carbon (DOC), riverine inorganic carbon

(IC) and outgassed carbon). The relative changes in POC and DOC show similar patterns (see Fig. S2), therefore exemplary POC is shown and discussed in detail.

2.3.1 Evaluation of potential future changes

Spatial effects of the two deforestation scenarios (GOV and BAU) on the different riverine carbon pools and fluxes have been estimated by calculating the common logarithm ($\log_{10}$) of the ratio of mean future (2070-2099) carbon amounts of the deforestation scenarios and mean future carbon amounts of the NatVeg scenario (E_{Defor}, Eq. (3)) for each simulation run.

$$E_{Defor} = log_{10} \frac{\sum_{t=2070}^{2099} C_{Defor_t}}{\sum_{t=2070}^{2099} C_{NatVeg_t}} \quad (3)$$

To estimate changes caused by the combination of climate change and deforestation $E_{CCDefor}$ compares future carbon pools in the deforestation scenarios to carbon pools during the reference period (1971-2000) in the NatVeg scenario (Eq. (4)).

$$E_{CCDefor} = log_{10} \frac{\sum_{t1=2070}^{2099} C_{Defor_{t1}}}{\sum_{t2=1971}^{2000} C_{NatVeg_{t2}}} \quad (4)$$

Each simulation run combines deforestation and emission scenarios and aggregates the outputs for all five climate model inputs used. To identify areas where the differences between values in the reference period and future values are significant (p-value <0.05), the Wilcoxon Rank Sum Test for not-normally distributed datasets (Bauer, 1972) has been applied for each cell.

Additionally to the spatial assessment, time series were deduced based on mean values over the entire basin and each of the three exemplary regions R1, R2 and R3. These means of the carbon pools were calculated for every year during the simulation period. Changes have been expressed as the five-year-running-mean of the quotient of annual future carbon amounts in the deforestation and in the NatVeg scenarios. These analyses have been conducted both for the whole Amazon basin and for three selected sub-regions.

2.3.2 Estimating the dominant driver for changes

We estimated which factor is causing the observed changes the most. To estimate the contribution of either climate change (D_{CC}, Eq. (5)) or deforestation (D_{Defor}, Eq. (6)), reference carbon amounts of the NatVeg scenario have been compared to future amounts of the NatVeg scenario (D_{CC}), and future carbon amounts of the NatVeg scenario have been compared to future amounts of the deforestation scenarios (D_{Defor}).

$$D_{CC} = \left| log_{10} \frac{\sum_{t1=2070}^{2099} C_{NatVeg_{t1}}}{\sum_{t2=1971}^{2000} C_{NatVeg_{t2}}} \right| \quad (5)$$

$$D_{Defor} = |E_{Defor}| \quad (6)$$

We define a cell as dominated by climate change effects, if $D_{CC}>D_{Defor}$ and dominated by deforestation effects if $D_{CC}<D_{Defor}$. The impact values D_{CC} and D_{Defor} ($median_{POC}$ = 0.9695, $median_{IC}$ = 1.0106, and $median_{outgassedC}$ = 0.9982) have been rounded to the second decimal place. If both values are equal, the two effects balance each other.

3 Results

3.1 Changes caused by deforestation

Deforestation decreases riverine particulate and dissolved organic carbon (POC and DOC). When continuing high deforestation rates as projected under the BAU deforestation scenario, the decrease in POC is more intense than under GOV deforestation rates (Figure 2A and Figure 2B; for DOC see Figs. S2A and S2B).In some highly deforested sites in the South-East of the basin the amount of POC is only 10% of the amount under no deforestation (indicated by E_{Defor}). This pattern is robust between the model realizations with a high agreement of the results amongst the five climate models. In the deforestation scenarios the changes in future POC are drastic, even though the difference between the three emission scenarios A1B, A2, and B1 are very small. However, in some regions within the Amazon basin POC increases (up to 3fold), especially in mountain regions (e.g. Andes and Guiana Shield). Although POC and DOC respond similar in relative terms (see Fig S2), the absolute amounts are approximately twice as high for DOC compared to POC (Table 2). The mean basin-wide loss in POC ranges between 0.13×10^{12} g yr^{-1} (A2) and 0.24×10^{12} g yr^{-1} (A1B) in the GOV scenario, and between 0.37×10^{12} g yr^{-1} (A2) and 0.48×10^{12} g yr^{-1} (A1B) in the BAU scenario. The SRES A2 scenario causes the largest changes in POC, further increasing the loss caused by deforestation.

Changes in outgassed riverine carbon caused by deforestation (Figure 2C and Figure 2D) show a similar pattern as the changes in POC, with an even clearer effect of deforestation on a larger area. In both scenarios deforestation decreases outgassed carbon to up to one tenth compared to the amount produced under the NatVeg scenario. The agreement between the five climate models is even larger than in POC. In contrast to the overall pattern, some areas in the Andes and the Guiana Shield show an increase in outgassed carbon of up to a factor of 30, but these areas are an exception. Like in POC the differences between the SRES scenarios are only minor. For the absolute values see Table 2.

For riverine inorganic carbon (IC) deforestation caused significant changes (E_{Defor}, p-value <0.05) only in small areas (Figure 2E and Figure 2F). In these regions, in the very South of the basin and in single spots in the North, i.e. in the headwaters of the watershed, IC increases by a factor of up to 1.2. Besides these areas of increase, a slight decrease of about 5% is simulated for the region along the main stem of the Amazon River, downstream of Manaus and along the Rio Madeira and the Rio Tapajós. In contrast to POC, the spatial pattern of change in IC does not obviously follow the deforestation patterns. Therefore, the differences between the two deforestation scenarios GOV and BAU scenarios are minor. Whereas POC,

DOC, and outgassed carbon show a clear decrease due to deforestation, IC shows a nearly neutral response with maximal mean basin-wide gains (for absolute values see Table 2).

3.2 Changes caused by a combination of deforestation and climate change

Climate change and deforestation together will lead to large overall changes in the amount of riverine and exported carbon. Riverine POC and DOC amounts will decrease by about 19.8% and 22.2%, respectively, and exported organic carbon will decrease by about 38.1% (Figure 3). In contrast riverine IC will increase by about 100%, combined with a slight increase of outgassed carbon by about 2.7% (Figure 3). In detail, the basin-wide changes in the amount of POC (Figure 4A-B and Figure 5A) caused by deforestation and climate change range between a 2.5-fold increase and a decrease to one tenth. The increase is mainly caused by climate change (indicated by the green cell borders in Figure 4), whereas the decrease is mainly caused by deforestation (red cell borders). The differences mainly induced by deforestation are larger in the BAU compared to the GOV scenario. In contrast, the differences caused by climate change show no large differences between the two deforestation scenarios. The differences between the emission scenarios are minor (see also Table 2). In some areas the dominance of forcing shifts from climate change dominance (D_{CC}) for the GOV scenario (green cell border) to deforestation dominance (D_{Defor}) for the BAU scenario (red cell border) due to the higher land use intensity as a result of deforestation (see also Table 3). While in the GOV scenario 20% of all cells are dominated by deforestation impacts, this value increases for the BAU scenario to 30%. During the first decades (2000-2030) basin-wide POC is partly larger in the deforestation scenarios than in the NatVeg scenario by up to 2% in 2000 and about 1% in 2020 (Figure 5A). All climate models show reduced POC amounts in the deforestation scenarios compared to the NatVeg scenario after 2040. The POC amount in the GOV deforestation scenario decreases gradually until the decrease levels off in the late 2060s, i.e. ten years after the constant deforestation area is kept constant. In the BAU scenario, POC decreases strongly in the 2040 to 2060s leading to a loss of about 25% compared to 10% in the GOV scenario.

The three sub-regions R1 to R3 show different patterns (Figure 5A). While in region R1 the difference in the POC amounts between the GOV and the BAU scenario is only small, reflecting the low deforestation in this region, the differences between the two deforestation scenarios are more explicit in regions R2 and especially in R3 (with the largest area deforested), where in addition model uncertainty is low. Starting in the 2050s, the variation between different emission scenarios and climate models increases. Alike the results of the impact of deforestation alone POC and DOC show a similar pattern (see also Table 2).

The changes in outgassed carbon (Figure 4C-D and Figure 5B) are in the same range as changes in POC. Climate change increases outgassed carbon by about 20%, especially in the North-Western basin (Figure 4C-D). The deforestation induces a decrease on outgassed carbon to one tenth in areas with high fraction of deforested area, i.e. in the Eastern and South-Eastern basin. Again, the differences in effects are much larger between the two deforestation scenarios (GOV vs. BAU) than between the different emission scenarios (see also Table 2). After 2050 the rate of deforestation determines the differences in the amount of outgassed carbon (Figure 5B) as well. The outgassed carbon directly depends on the available

POC, therefore the time series of both, POC and IC widely match. Under the GOV scenario the basin-wide loss of outgassed carbon is about 16% towards the end of the century. The results of the BAU scenario show an average loss of outgassed carbon of 28%.

Changes in inorganic carbon (IC) are mainly driven by climate change (under all emission scenarios), less by the magnitude of deforestation (Figure 4E-F and Figure 5C, Tables 2 and 3). In about half of the Amazon basin the IC amount significantly changes due to climate change (insignificant changes in the other 50%), but in no cell due to deforestation. The magnitude of change varies between emission scenarios: the increase in IC is up to 4-fold in the A2 scenario and up to 2.5-fold in the B1 scenario (see Table 2). For both deforestation scenarios the gain of IC is dominant until 2050, while the basin-wide trend becomes unclear afterwards. However, sub-regions like R1 and R3 show a slight increase during the whole century (Figure 5C).

4 Discussion

Deforestation is, besides climate change, the largest threat to Amazonia. It leads directly to a decrease in terrestrial biomass and an increase in CO_2 emissions (Potter et al., 2009) and has indirect effects on aquatic biomass, diversity of species and their habitats and the climate (Asner and Alencar, 2010; Bernardes et al., 2004; Costa et al., 2003). Our results show that deforestation is also likely to changes the amount of riverine organic carbon as well as exported carbon.

We identified a basin-wide reduction in riverine particulate and dissolved organic carbon pools by about 10% to 25% by the end of this century (Figure 5). This reduction is particularly pronounced in areas of high deforestation intensity at the *Arc of Deforestation*, at the Rio Madeira and the last 500 km stretch of the Rio Amazon, where terrestrial carbon is most intensively reduced. In the first decades of the 21st century the differences in carbon amounts between the two deforestation scenarios are only small (Figure 5). During these decades the deforestation-induced increase in discharge (as reported by Costa et al., 2003) is able to partly compensate the decreasing amount of terrigenous organic matter which is the source of riverine organic matter. After the 2050s, the differences in the organic carbon pools caused by deforestation become more obvious (Figure 5), with larger carbon decrease under the more severe BAU scenario. The same patterns occur in the two regions with the pronounced deforestation (R1 and R2). Here the reduction of terrestrial carbon directly reduces the amount of riverine carbon. The variation in future riverine carbon fluxes within each deforestation scenario can be attributed to the differences climate projections and emission scenarios, especially after 2060 when deforested area remains constant and the lagged deforestation effects vanish. In regions with low deforestation intensity (i.e. R1) the effects of land use change are much smaller and the climate change effects dominate the change in riverine organic carbon and outgassed carbon.

The reduction in the riverine organic carbon pools will have consequences for the floodplain and the river itself. Floodplains as well as riverine biotopes depend on the annually recurring

input of organic material, either as food supply or fertilizer (Junk and Wantzen, 2004). The productivity of the floodplain forests is mainly driven by the input of nutrients which are basically sediments and organic material (Worbes, 1997). While the sediment input (also adding nutrients) might increase due to increased discharge, the input of organic material from upstream areas will decrease, leading to a reduced terrestrial and riverine productivity. This reduced productivity will certainly impact many animal species that rely on the food supplied by trees, such as fruits or leaves. The reduced supply of fertilizer and food will therefore likely affect plant and animal species compositions on local and regional scales (Junk and Wantzen, 2004; Worbes, 1997).

Additionally, deforestation will have secondary effects, including a reduction in evasion of CO_2 from the water (outgassed carbon). Lower terrestrial productivity after deforestation decreases the organic carbon material in the river and thus also the respiration to CO_2. This is opposed by the higher respiration rate as a result of increased temperatures due to climate change. These indirect effects of deforestation on riverine carbon dynamics have to be included in future carbon balance estimates of the sink/source behaviour of the Amazon basin, since it directly couples the change in land use to the atmospheric, marine and therefore global carbon fluxes.

In contrast to the amount of riverine organic carbon and outgassed carbon the amount of riverine inorganic carbon does not show a significant effect of deforestation. Climate change-induced higher water temperature causes a reduction in solubility of CO_2, and higher atmospheric CO_2 concentrations lead to an increase in dissolved CO_2. The combination of both effects leads to a slight increase in dissolved inorganic carbon in the beginning and a neutral signal towards the end of the century independently of the deforestation.

The deforestation of tropical forests will not only affect processes within the rainforest, but also processes in the adjacent Atlantic Ocean. Currently, the annual export of about 6,300 km^3 of freshwater is accompanied by 40×10^{12} g of organic carbon to the Atlantic Ocean (Gaillardet et al., 1997; Moreira-Turcq et al., 2003). The present study shows that deforestation leads to a reduction in the exported organic carbon to the ocean by approximately 40%. In the NatVeg scenario the proportion of exported organic carbon to the ocean makes up about 0.8-0.9% of the net primary productions (NPP), whereas in the heavily deforested BAU scenario this proportion is reduced to about 0.5-0.6%. The reduction in the ratio of exported carbon to NPP by deforestation indicates a less pronounced future sink, since the organic carbon is directly extracted from the forest and additionally indirectly from the ocean. Globally about 60×10^{15}g of carbon per year are fixed by the terrestrial vegetation as net primary productivity. After heterotrophic respiration about 6×10^{15} g of carbon per year are sequestered in the ecosystem. In central Amazonia net primary production sums up to about 1×10^{9} g C km^{-2} yr^{-1} (Malhi et al., 2009). The Amazon basin is considered a carbon sink (Lewis et al., 2011). Our results show that riverine carbon dynamics likely add another 146×10^{12}g yr^{-1} in terms of carbon outgassed from the Amazon basin and 33.6×10^{12}g yr^{-1} exported to the Atlantic Ocean under the combined effect of climate change and deforestation (202×10^{12}g C yr^{-1} and 54.9×10^{12}g C yr^{-1}, respectively, under climate change only). Therefore, future assessments of climate-change and

deforestation-induced changes on the carbon balance of the Amazon basin have to include the amount of carbon exported to the ocean and outgassed from the river basin to the atmosphere.

The import of organic material to the ocean positively impacts the respiration and production of the Atlantic Ocean off the coast of South America (Körtzinger, 2003; Cooley and Yager, 2006; Cooley et al., 2007; Subramaniam et al., 2008). A reduction of the import might therefore reduce the productivity in the coast-near ocean since these costal zones depend on the imported organic matter (Cooley and Yager, 2006; Körtzinger, 2003; Subramaniam et al., 2008) and might have further impacts along the trophic cascade including herbivorous and piscivorous fish. Besides the reduced organic carbon, higher amounts of nutrients may be imported to the ocean, because the nutrients are only marginally taken up within the river and by the former intact adjacent forests. The imports of both, less organic carbon and more nutrients, might induce changes in oceanic heterotrophy and primary production.

4.1 Shortcomings of the approach

The strong decrease of organic carbon may be overestimated because of our model assumptions, which include a complete removal of the natural vegetation carbon during deforestation (see e.g. Figure 5). In reality, the complete conversion of the floodplain forests to cropland or pasture is not very likely. In the more severe deforestation scenario (BAU) about 6% of the area is deforested (Soares-Filho et al., 2006). In our scenarios this also includes areas which are temporarily flooded. Since temporarily inundated areas cannot be easily converted to agricultural area or settlements, this might lead to an overestimation of deforested area. But, for example in Manaus, floodplains within a radius of about 500 km around the city have been extensively logged for construction purposes between 1960 and 1980 (Goulding et al., 2003).

In our study deforestation is simulated by partial or complete removal of vegetation carbon. This also reduces the litter and soil carbon through respiration over time, since these carbon pools are not refilled by litter fall from the vegetation, as they would do in reality by the dead organic material generated by the crops and managed land that replaced the natural vegetation. Therefore, our estimates represent more drastic changes in riverine carbon dynamics than would likely occur if carbon export from managed land would be considered. Because the deforested cell fraction has been kept constant from 2050 to 2099 the results show how carbon pools stabilize after the 2050s. The sharp decrease in POC and outgassed carbon after 2050, as it is one result of our study, is caused by the implementation of carbon removal in the model. During inundation the cells are partly or completely covered with water, which leads to the export of organic material. After the gradual decrease of forest cover (and therewith input of organic material) before 2050, there is a depletion of the remaining organic material in the following years. By a more gradual implementation of inundation in the model this harsh decrease would be softened.

In this study the mobilization of terrigenous organic material is exclusively controlled by inundation. A model that also considers the impact of precipitation, vegetation cover and slope on erosion would likely lead to an increase in erosion and thus to the import of organic

matter to the river (McClain and Elsenbeer, 2001) in the first years after deforestation. However, this additional influx of carbon would only be temporal, since the soil and litter carbon pools would be eroded after some years (McClain and Elsenbeer, 2001). Thus, we assume that for the investigation of the long-term dynamics of carbon pools and fluxes, such erosion effects are only of minor importance.

5 Conclusion

Deforestation decreases terrestrial biomass and contributes to a further increase in CO_2 emissions, which reduces the terrestrial carbon sequestration potential (Houghton et al., 2000; Potter et al., 2009). Moreover, our results show that deforestation will lead to a significant decrease of exported terrigenous organic carbon, leading to a reduction of the amount of riverine organic carbon. The climate change effects additionally increase in the amount of riverine inorganic carbon. Deforestation further decreases the amount of riverine organic carbon leading to a combined decrease by about 20% compared to 10% under climate change alone (Langerwisch et al. 2015). While climate change alone leaves the export to the Atlantic Ocean with +1% nearly unchanged (Langerwisch et al. 2015), considering deforestation will now decrease the export of organic carbon to the ocean by about 40%. In contrast climate change will strongly increase the outgassed carbon by about 40% (Langerwisch et al. 2015), but including deforestation will reduces this increase to only +3%.

These changes in the hydrological regimes and the fluvial carbon pools might add to the pressures that are being imposed on the Amazon ecosystems (Asner et al., 2006; Asner and Alencar, 2010), with strong consequences for ecosystem stability (Brown and Lugo, 1990; Foley et al., 2002; von Randow et al., 2004). For instance, fish play a key role in seed dispersal along the Amazon. If floodplains turn into less productive grounds for juvenile fish, these changes might have considerable effects on local vegetation recruitment dynamics and regional plant biodiversity (Horn et al., 2011). We therefore strongly advocate the combined terrestrial and fluvial perspective of our approach, and its ability to address both climate and land use change.

Acknowledgements. We thank “Pakt für Forschung der Leibniz-Gemeinschaft” for funding the TRACES project for FL. AR was funded by FP7 AMAZALERT (Project ID 282664) and Helmholtz Alliance ‘Remote Sensing and Earth System Dynamics’. We also thank Susanne Rolinski and Dieter Gerten for discussing the hydrological aspects. We thank Alice Boit for fruitful comments on the manuscript. Additionally we thank our LPJmL and ECOSTAB colleagues at PIK for helpful comments on the design of the study and the manuscript. We also thank the anonymous reviewers and the handling editor whose comments and suggestions greatly improved the manuscript.

Author contributions. Model development: FL, BT, WC. Data analysis: FL, AR, KT. Drafting the article: FL, AW, BT, AR, KT.

6 References

Aguiar, A. P. D., Vieira, I. C. G., Assis, T. O., Dalla-Nora, E. L., Toledo, P. M., Oliveira Santos-Junior, R. A., Batistella, M., Coelho, A. S., Savaget, E. K., Aragão, L. E. O. C., Nobre, C. A. and Ometto, J. P. H.: Land use change emission scenarios: anticipating a forest transition process in the Brazilian Amazon, Global Change Biology, 22(5), 1821–1840, doi:10.1111/gcb.13134, 2016.

Anderson, J. T., Nuttle, T., Saldaña Rojas, J. S., Pendergast, T. H. and Flecker, A. S.: Extremely long-distance seed dispersal by an overfished Amazonian frugivore, Proceedings of the Royal Society B: Biological Sciences, 278, 3329–3335, doi:10.1098/rspb.2011.0155, 2011.

Asner, G. P. and Alencar, A.: Drought impacts on the Amazon forest: the remote sensing perspective, New Phytologist, 187(3), 569–578, doi:10.1111/j.1469-8137.2010.03310.x, 2010.

Asner, G. P., Broadbent, E. N., Oliveira, P. J. C., Keller, M., Knapp, D. E. and Silva, J. N. M.: Condition and fate of logged forests in the Brazilian Amazon, Proceedings of the National Academy of Sciences, 103(34), 12947–12950, 2006.

Bauer, D. F.: Constructing confidence sets using rank statistics, Journal of the American Statistical Association, 67(339), 687–690, 1972.

Bernardes, M. C., Martinelli, L. A., Krusche, A. V., Gudeman, J., Moreira, M., Victoria, R. L., Ometto, J. P. H. B., Ballester, M. V. R., Aufdenkampe, A. K., Richey, J. E. and Hedges, J. I.: Riverine organic matter composition as a function of land use changes, Southwest Amazon, Ecological Applications, 14(4), S263–S279, doi:10.1890/01-6028, 2004.

Biemans, H., Hutjes, R. W. A., Kabat, P., Strengers, B. J., Gerten, D. and Rost, S.: Effects of precipitation uncertainty on discharge calculations for main river basins, Journal of Hydrometeorology, 10(4), 1011–1025, doi:10.1175/2008jhm1067.1, 2009.

Bondeau, A., Smith, P. C., Zaehle, S., Schaphoff, S., Lucht, W., Cramer, W., Gerten, D., Lotze-Campen, H., Müller, C., Reichstein, M. and Smith, B.: Modelling the role of agriculture for the 20th century global terrestrial carbon balance, Global Change Biology, 13(3), 679–706, doi:10.1111/j.1365-2486.2006.01305.x, 2007.

Brown, S. and Lugo, A. E.: Tropical secondary forests, Journal of Tropical Ecology, 6(1), 1–32, 1990.

Collatz, G. J., Ribas-Carbo, M. and Berry, J. A.: Coupled photosynthesis-stomatal conductance model for leaves of C4 plants, Functional Plant Biology, 19(5), 519–538, doi:10.1071/PP9920519, 1992.

Cooley, S. R. and Yager, P. L.: Physical and biological contributions to the western tropical North Atlantic Ocean carbon sink formed by the Amazon River plume, Journal of Geophysical Research-Oceans, 111(C08018), doi:10.1029/2005JC002954, 2006.

564 Cooley, S. R., Coles, V. J., Subramaniam, A. and Yager, P. L.: Seasonal variations in the
565 Amazon plume-related atmospheric carbon sink, Global Biogeochemical Cycles, 21(3),
566 doi:10.1029/2006GB002831, 2007.

567 Costa, M. H., Botta, A. and Cardille, J. A.: Effects of large-scale changes in land cover on the
568 discharge of the Tocantins River, Southeastern Amazonia, Journal of Hydrology, 283(1–4),
569 206–217, doi:10.1016/S0022-1694(03)00267-1, 2003.

570 Costa, M. H., Yanagi, S. N. M., Souza, P., Ribeiro, A. and Rocha, E. J. P.: Climate change in
571 Amazonia caused by soybean cropland expansion, as compared to caused by pastureland
572 expansion, Geophysical Research Letters, 34(7), doi:10.1029/2007GL029271, 2007.

573 Cramer, W., Bondeau, A., Woodward, F. I., Prentice, I. C., Betts, R. A., Brovkin, V., Cox, P.
574 M., Fisher, V., Foley, J. A., Friend, A. D., Kucharik, C., Lomas, M. R., Ramankutty, N.,
575 Sitch, S., Smith, B., White, A. and Young-Molling, C.: Global response of terrestrial
576 ecosystem structure and function to CO_2 and climate change: results from six dynamic global
577 vegetation models, Global Change Biology, 7(4), 357–373, 2001.

578 Eva, H. D., Belward, A. S., De Miranda, E. E., Di Bella, C. M., Gond, V., Huber, O., Jones,
579 S., Sgrenzaroli, M. and Fritz, S.: A land cover map of South America, Global Change
580 Biology, 10(5), 731–744, 2004.

581 Fader, M., Rost, S., Müller, C., Bondeau, A. and Gerten, D.: Virtual water content of
582 temperate cereals and maize: Present and potential future patterns, Journal of Hydrology,
583 384(3–4), 218–231, doi:10.1016/j.jhydrol.2009.12.011, 2010.

584 Farquhar, G. D., van Caemmerer, S. and Berry, J. A.: A biochemical model of photosynthetic
585 CO_2 assimilation in leaves of C3 species, Planta, 149, 78–90, 1980.

586 Fearnside, P. M.: Environment: Deforestation soars in the Amazon, Nature, 521(7553), 423–
587 423, doi:10.1038/521423b, 2015.

588 Foley, J. A., Botta, A., Coe, M. T. and Costa, M. H.: El Niño-Southern Oscillation and the
589 climate, ecosystems and rivers of Amazonia, Global Biogeochemical Cycles, 16(4), 79/1-
590 79/17, doi:10.1029/2002GB001872, 2002.

591 Foley, J. A., Asner, G. P., Costa, M. H., Coe, M. T., DeFries, R., Gibbs, H. K., Howard, E. A.,
592 Olson, S., Patz, J., Ramankutty, N. and Snyder, P.: Amazonia revealed: forest degradation and
593 loss of ecosystem goods and services in the Amazon Basin, Frontiers in Ecology and the
594 Environment, 5(1), 25–32, doi:10.1890/1540-9295(2007)5[25:ARFDAL]2.0.CO;2, 2007.

595 Gaillardet, J., Dupré, B., Allègre, C. J. and Négrel, P.: Chemical and physical denudation in
596 the Amazon River basin, Chemical Geology, 142(3–4), 141–173, 1997.

597 Gerten, D., Schaphoff, S., Haberlandt, U., Lucht, W. and Sitch, S.: Terrestrial vegetation and
598 water balance - hydrological evaluation of a dynamic global vegetation model, Journal of
599 Hydrology, 286(1–4), 249–270, doi:10.1016/j.jhydrol.2003.09.029, 2004.

600 Gerten, D., Rost, S., von Bloh, W. and Lucht, W.: Causes of change in 20th century global
601 river discharge, Geophysical Research Letters, 35(20), doi:L20405 10.1029/2008gl035258,
602 2008.

603 Godar, J., Gardner, T. A., Tizado, E. J. and Pacheco, P.: Actor-specific contributions to the
604 deforestation slowdown in the Brazilian Amazon, Proceedings of the National Academy of
605 Sciences, 111(43), 15591–15596, doi:10.1073/pnas.1322825111, 2014.

606 Gordon, W. S., Famiglietti, J. S., Fowler, N. L., Kittel, T. G. F. and Hibbard, K. A.:
607 Validation of simulated runoff from six terrestrial ecosystem models: results from VEMAP,
608 Ecological Applications, 14(2), 527–545, doi:10.1890/02-5287, 2004.

609 Goulding, M., Barthem, R. and Ferreira, E.: The Smithsonian Atlas of the Amazon,
610 Smithsonian, Washington and London., 2003.

611 Hamilton, S. K.: Biogeochemical implications of climate change for tropical rivers and
612 floodplains, Hydrobiologia, 657(1), 19–35, doi:10.1007/s10750-009-0086-1, 2010.

613 Hedges, J. I., Mayorga, E., Tsamakis, E., McClain, M. E., Aufdenkampe, A., Quay, P.,
614 Richey, J. E., Benner, R., Opsahl, S., Black, B., Pimentel, T., Quintanilla, J. and Maurice, L.:
615 Organic matter in Bolivian tributaries of the Amazon River: A comparison to the lower
616 mainstream, Limnology and Oceanography, 45(7), 1449–1466, 2000.

617 Hoorn, C., Wesselingh, F. P., ter Steege, H., Bermudez, M. A., Mora, A., Sevink, J.,
618 Sanmartin, I., Sanchez-Meseguer, A., Anderson, C. L., Figueiredo, J. P., Jaramillo, C., Riff,
619 D., Negri, F. R., Hooghiemstra, H., Lundberg, J., Stadler, T., Sarkinen, T. and Antonelli, A.:
620 Amazonia through time: Andean uplift, climate change, landscape evolution, and biodiversity,
621 Science, 330(6006), 927–931, doi:10.1126/science.1194585, 2010.

622 Horn, M. H., Correa, S. B., Parolin, P., Pollux, B. J. A., Anderson, J. T., Lucas, C., Widmann,
623 P., Tjiu, A., Galetti, M. and Goulding, M.: Seed dispersal by fishes in tropical and temperate
624 fresh waters: The growing evidence, Acta Oecologica, 37, 561–577,
625 doi:10.1016/j.actao.2011.06.004, 2011.

626 Houghton, R. A., Skole, D. L., Nobre, C. A., Hackler, J. L., Lawrence, K. T. and
627 Chomentowski, W. H.: Annual fluxes or carbon from deforestation and regrowth in the
628 Brazilian Amazon, Nature, 403(6767), 301–304, 2000.

629 Houghton, R. A., Lawrence, K. T., Hackler, J. L. and Brown, S.: The spatial distribution of
630 forest biomass in the Brazilian Amazon: a comparison of estimates, Global Change Biology,
631 7(7), 731–746, 2001.

632 INPE: Projeto PRODES: Monitoramento da floresta Amazônica Brasileira por satélite.
633 [online] Available from: http://www.obt.inpe.br/prodes/index.php (Accessed 28 April 2015),
634 2013.

635 Irmler, U.: Litterfall and nitrogen turnover in an Amazonian blackwater inundation forest,
636 Plant and Soil, 67(1–3), 355–358, 1982.

637 Johnson, M. S., Lehmann, J., Selva, E. C., Abdo, M., Riha, S. and Couto, E. G.: Organic
638 carbon fluxes within and streamwater exports from headwater catchments in the southern
639 Amazon, Hydrological Processes, 20(12), 2599–2614, 2006.

640 Junk, W. J.: The central Amazon floodplain - Ecology of a pulsing system, Springer., 1997.

641 Junk, W. J. and Wantzen, K. M.: The flood pulse concept: New aspects, approaches and
642 applications - An update, in Proceedings of the Second International Symposium on the

643 Management of large Rivers for Fisheries, edited by R. L. Welcomme and T. Petr, pp. 117–
644 140., 2004.

645 Jupp, T. E., Cox, P. M., Rammig, A., Thonicke, K., Lucht, W. and Cramer, W.: Development
646 of probability density functions for future South American rainfall, New Phytologist, 187,
647 682–693, doi:10.1111/j.1469-8137.2010.03368.x, 2010.

648 Keller, M., Bustamante, M., Gash, J. and Silva Dias, P., Eds.: Amazonia and global change,
649 American Geophysical Union, Washington, DC., 2009.

650 Körtzinger, A.: A significant CO_2 sink in the tropical Atlantic Ocean associated with the
651 Amazon River plume, Geophysical Research Letters, 30(24), doi:10.1029/2003GL018841,
652 2003.

653 Langerwisch, F., Rost, S., Gerten, D., Poulter, B., Rammig, A. and Cramer, W.: Potential
654 effects of climate change on inundation patterns in the Amazon Basin, Hydrology and Earth
655 System Sciences, 17(6), 2247–2262, doi:10.5194/hess-17-2247-2013, 2013.

656 Langerwisch, F., Walz, A., Rammig, A., Tietjen, B., Thonicke, K. and Cramer, W.: Climate
657 change increases riverine carbon outgassing while export to the ocean remains uncertain,
658 Earth System Dynamics Discussions, 6(2), 1445–1497, doi:10.5194/esdd-6-1445-2015, 2015.

659 Lawrence, D. and Vandecar, K.: Effects of tropical deforestation on climate and agriculture,
660 Nature Climate Change, 5(1), 27–36, doi:10.1038/nclimate2430, 2014.

661 Lewis, S. L., Brando, P. M., Phillips, O. L., van der Heijden, G. M. . and Nepstad, D.: The
662 2010 amazon drought, Science, 331(6017), 554, doi:10.1126/science.1200807, 2011.

663 Malhi, Y., Wood, D., Baker, T. R., Wright, J., Phillips, O. L., Cochrane, T., Meir, P., Chave,
664 J., Almeida, S., Arroyo, L., Higuchi, N., Killeen, T. J., Laurance, S. G., Laurance, W. F.,
665 Lewis, S. L., Monteagudo, A., Neill, D. A., Vargas, P. N., Pitman, N. C. A., Quesada, C. A.,
666 Salomão, R., Silva, J. N. M., Lezama, A. T., Terborgh, J., Martínez, R. V. and Vinceti, B.:
667 The regional variation of aboveground live biomass in old-growth Amazonian forests, Global
668 Change Biology, 12(7), 1107–1138, 2006.

669 Malhi, Y., Roberts, J. T., Betts, R. A., Killeen, T. J., Li, W. and Nobre, C. A.: Climate change,
670 deforestation, and the fate of the Amazon, Science, 319(5860), 169–172, 2008.

671 Malhi, Y., Saatchi, S., Girardin, C. and Aragão, L. E. O. C.: The production, storage, and flow
672 of carbon in Amazonian forests, in Amazonia and Global Change, pp. 355–372, American
673 Geophysical Union, Washington, DC., 2009.

674 Mayorga, E., Aufdenkampe, A. K., Masiello, C. A., Krusche, A. V., Hedges, J. I., Quay, P.
675 D., Richey, J. E. and Brown, T. A.: Young organic matter as a source of carbon dioxide
676 outgassing from Amazonian rivers, Nature, 436(7050), 538–541, doi:10.1038/nature03880,
677 2005.

678 McClain, M. E. and Elsenbeer, H.: Terrestrial inputs to Amazon streams and internal
679 biogeochemical processing, in The Biogeochemistry of the Amazon Basin, edited by M. E.
680 McClain, R. L. Victoria, and J. E. Richey, pp. 185–208, Oxford University Press, New York.,
681 2001.

Melack, J. M. and Forsberg, B.: Biogeochemistry of Amazon floodplain lakes and associated wetlands, in The Biogeochemistry of the Amazon Basin and its Role in a Changing World, pp. 235–276, Oxford University Press, Eds. McClain, M. E.; Victoria, R. L.; Richey, J. E., 2001.

Moreira-Turcq, P., Seyler, P., Guyot, J. L. and Etcheber, H.: Exportation of organic carbon from the Amazon River and its main tributaries, Hydrological Processes, 17(7), 1329–1344, doi:10.1002/hyp.1287, 2003.

Nakićenović, N., Davidson, O., Davis, G., Grübler, A., Kram, T., Lebre La Rovere, E., Metz, B., Morita, T., Pepper, W., Pitcher, H., Sankovski, A., Shukla, P., Swart, R. and Dadi, Z.: IPCC Special report on emission scenarios, [online] Available from: http://www.ipcc.ch/ipccreports/sres/emission/index.php?idp=0, 2000.

Nepstad, D., McGrath, D., Stickler, C., Alencar, A., Azevedo, A., Swette, B., Bezerra, T., DiGiano, M., Shimada, J., Seroa da Motta, R., Armijo, E., Castello, L., Brando, P., Hansen, M. C., McGrath-Horn, M., Carvalho, O. and Hess, L.: Slowing Amazon deforestation through public policy and interventions in beef and soy supply chains, Science, 344(6188), 1118–1123, doi:10.1126/science.1248525, 2014.

Nobre, A. D.: The Future Climate of Amazonia: Scientific Assessment Report, INPA and ARA, São José dos Campos, Brazil. [online] Available from: http://www.ccst.inpe.br/wp-content/uploads/2014/11/ The_Future_Climate_of_Amazonia_Report.pdf (Accessed 31 August 2015), 2014.

Poorter, L., Bongers, F., Aide, T. M., Almeyda Zambrano, A. M., Balvanera, P., Becknell, J. M., Boukili, V., Brancalion, P. H. S., Broadbent, E. N., Chazdon, R. L., Craven, D., de Almeida-Cortez, J. S., Cabral, G. A. L., de Jong, B. H. J., Denslow, J. S., Dent, D. H., DeWalt, S. J., Dupuy, J. M., Durán, S. M., Espírito-Santo, M. M., Fandino, M. C., César, R. G., Hall, J. S., Hernandez-Stefanoni, J. L., Jakovac, C. C., Junqueira, A. B., Kennard, D., Letcher, S. G., Licona, J.-C., Lohbeck, M., Marín-Spiotta, E., Martínez-Ramos, M., Massoca, P., Meave, J. A., Mesquita, R., Mora, F., Muñoz, R., Muscarella, R., Nunes, Y. R. F., Ochoa-Gaona, S., de Oliveira, A. A., Orihuela-Belmonte, E., Peña-Claros, M., Pérez-García, E. A., Piotto, D., Powers, J. S., Rodríguez-Velázquez, J., Romero-Pérez, I. E., Ruíz, J., Saldarriaga, J. G., Sanchez-Azofeifa, A., Schwartz, N. B., Steininger, M. K., Swenson, N. G., Toledo, M., Uriarte, M., van Breugel, M., van der Wal, H., Veloso, M. D. M., Vester, H. F. M., Vicentini, A., Vieira, I. C. G., Bentos, T. V., Williamson, G. B. and Rozendaal, D. M. A.: Biomass resilience of Neotropical secondary forests, Nature, 530(7589), 211–214, doi:10.1038/nature16512, 2016.

Potter, C., Klooster, S. and Genovese, V.: Carbon emissions from deforestation in the Brazilian Amazon Region, Biogeosciences, 6(11), 2369–2381, 2009.

Randall, D. A., Wood, R. A., Bony, S., Colman, R., Fichefet, T., Fyfe, J., Kattsov, V., Pitman, A., Shukla, J., Srinivasan, J., Stouffer, R. J., Sumi, A. and Taylor, K. E.: Climate models and their evaluation, in Climate Change 2007: The Physical Science Basis. Contribution of Working Group I to the Fourth Assessment Report of the Intergovernmental Panel on Climate Change, edited by S. Solomon, D. Qin, M. Manning, Z. Chen, M. Marquis, K. B. Averyt, M. Tignor, and H. L. Miller, Cambridge University Press., 2007.

von Randow, C., Manzi, A. O., Kruijt, B., de Oliveira, P. J., Zanchi, F. B., Silva, R. L., Hodnett, M. G., Gash, J. H. C., Elbers, J. A., Waterloo, M. J., Cardoso, F. L. and Kabat, P.:

726 Comparative measurements and seasonal variations in energy and carbon exchange over
727 forest and pasture in South West Amazonia, Theoretical and Applied Climatology, 78(1–3),
728 5–26, doi:10.1007/s00704-004-0041-z, 2004.

729 Richey, J. E., Melack, J. M., Aufdenkampe, A. K., Ballester, V. M. and Hess, L. L.:
730 Outgassing from Amazonian rivers and wetlands as a large tropical source of atmospheric
731 CO_2, Nature, 416(6881), 617–620, doi:10.1038/416617a, 2002.

732 Rost, S., Gerten, D., Bondeau, A., Lucht, W., Rohwer, J. and Schaphoff, S.: Agricultural
733 green and blue water consumption and its influence on the global water system, Water
734 Resources Research, 44(9), doi:W09405 10.1029/2007wr006331, 2008.

735 Salimon, C. I., Davidson, E. A., Victoria, R. L. and Melo, A. W. F.: CO_2 flux from soil in
736 pastures and forests in southwestern Amazonia, Global Change Biology, 10(5), 833–843,
737 2004.

738 Sitch, S., Smith, B., Prentice, I. C., Arneth, A., Bondeau, A., Cramer, W., Kaplan, J. O.,
739 Levis, S., Lucht, W., Sykes, M. T., Thonicke, K. and Venevsky, S.: Evaluation of ecosystem
740 dynamics, plant geography and terrestrial carbon cycling in the LPJ dynamic global
741 vegetation model, Global Change Biology, 9(2), 161–185, doi:10.1046/j.1365-
742 2486.2003.00569.x, 2003.

743 Soares-Filho, B. S., Nepstad, D. C., Curran, L. M., Cerqueira, G. C., Garcia, R. A., Ramos, C.
744 A., Voll, E., McDonald, A., Lefebvre, P. and Schlesinger, P.: Modelling conservation in the
745 Amazon basin, Nature, 440(7083), 520–523, 2006.

746 Spracklen, D. V., Arnold, S. R. and Taylor, C. M.: Observations of increased tropical rainfall
747 preceded by air passage over forests, Nature, 489(7415), 282–285, doi:10.1038/nature11390,
748 2012.

749 Subramaniam, A., Yager, P. L., Carpenter, E. J., Mahaffey, C., Bjorkman, K., Cooley, S.,
750 Kustka, A. B., Montoya, J. P., Sanudo-Wilhelmy, S. A., Shipe, R. and Capone, D. G.:
751 Amazon River enhances diazotrophy and carbon sequestration in the tropical North Atlantic
752 Ocean, Proceedings of the National Academy of Sciences, 105(30), 10460–10465,
753 doi:10.1073/pnas.0710279105, 2008.

754 Thonicke, K., Spessa, A., Prentice, I. C., Harrison, S. P., Dong, L. and Carmona-Moreno, C.:
755 The influence of vegetation, fire spread and fire behaviour on biomass burning and trace gas
756 emissions: results from a process-based model, Biogeosciences, 7(6), 1991–2011,
757 doi:10.5194/bg-7-1991-2010, 2010.

758 Wagner, W., Scipal, K., Pathe, C., Gerten, D., Lucht, W. and Rudolf, B.: Evaluation of the
759 agreement between the first global remotely sensed soil moisture data with model and
760 precipitation data, Journal of Geophysical Research, 108(4611), doi:10.1029/2003JD003663,
761 2003.

762 Waterloo, M. J., Oliveira, S. M., Drucker, D. P., Nobre, A. D., Cuartas, L. A., Hodnett, M. G.,
763 Langedijk, I., Jans, W. W. P., Tomasella, J., de Araújo, A. C., Pimentel, T. P. and Estrada, J.
764 C. M.: Export of organic carbon in run-off from an Amazonian rainforest blackwater
765 catchment, Hydrological Processes, 20(12), 2581–2597, 2006.

766 Worbes, M.: The forest ecosystem of the floodplains, in The Central Amazon Floodplain,
767 edited by W. J. Junk, pp. 223–265, Springer, Berlin, Germany., 1997.

768

769

7 Tables

Table 1: Location and characteristics of the three sub-regions.

	North-West corner	*South-East corner*	*area [$10^3 km^2$]*	*changes in inundation length*[*]	*changes inundated area*[*]	*land use intensity*
R1	0.5°S / 78.5°W	7.0°S / 72°W	523.03	1 month longer	larger	low
R2	1.0°S / 70.0°W	5.0°S / 52°W	891.32	±½ month shift	heterogeneous	medium
R3	4.5°S / 58.0°W	11.0°S / 52°W	523.03	½ month shorter	smaller	high

Regions are depicted in Figure S1. [*] Changes in inundation compared to the average of 1961-1990, as estimated and discussed in Langerwisch et al. (2013)

Table 2: Basin-wide (B) and region wise (R1-R3) amount of carbon in POC and DOC, outgassed carbon and IC [10^{12} g month^{-1}] averaged over 30 years and five climate models.

	$NatVeg_{ref}$	$NatVeg_{fut}$	GOV_{futA1B}	BAU_{futA1B}	GOV_{futA2}	BAU_{futA2}	GOV_{futB1}	BAU_{futB1}
POC								
B	1.64±0.06	1.76±0.51	1.52±0.43	1.28±0.35	1.63±0.41	1.39±0.34	1.55±0.31	1.30±0.24
R1	0.16±0.01	0.22±0.05	0.20±0.05	0.20±0.05	0.21±0.05	0.21±0.05	0.18±0.02	0.18±0.02
R2	0.42±0.01	0.43± 0.15	0.37±0.12	0.30±0.09	0.40±0.13	0.33±0.10	0.38±0.09	0.31±0.07
R3	0.15±0.01	0.14±0.05	0.11±0.04	0.07±0.03	0.12±0.04	0.08±0.02	0.12±0.03	0.08±0.02
DOC								
B	3.41±0.13	3.58±1.05	3.07±0.87	2.59±0.71	3.29±0.84	2.77±0.69	3.15±0.63	2.64±0.48
R1	0.34±0.02	0.46±0.11	0.43±0.10	0.42±0.10	0.45±0.10	0.44±0.10	0.39±0.05	0.38±0.05
R2	0.93±0.03	0.91±0.32	0.77±0.26	0.64±0.20	0.84±0.27	0.69±0.21	0.81±0.20	0.66±0.15
R3	0.34±0.02	0.30±0.11	0.24±0.09	0.16±0.06	0.26±0.08	0.17±0.05	0.27±0.07	0.17±0.04
outgassed carbon								
B	11.82±0.41	16.63±4.14	14.30±3.44	12.05±2.76	15.75±3.43	13.24±2.80	13.37±2.20	11.15±1.68
R1	1.15±0.06	2.05±0.38	1.93±0.35	1.91±0.35	2.10±0.35	2.08±0.35	1.61±0.13	1.60±0.14
R2	2.52±0.08	3.36±0.99	2.81±0.78	2.37±0.6	3.09±0.85	2.59±0.66	2.66±0.56	2.22±0.43
R3	0.99±0.04	1.12±0.42	0.91±0.34	0.55±0.20	1.03±0.32	0.62±0.18	0.94±0.26	0.56±0.14
IC								
B	0.227±0.003	0.457±0.119	0.457±0.120	0.456±0.121	0.523±0.137	0.522±0.138	0.365±0.063	0.364±0.064
R1	0.005±0.001	0.016±0.003	0.013±0.003	0.013±0.003	0.015±0.004	0.015±0.004	0.009±0.001	0.009±0.001
R2	0.153±0.002	0.308±0.081	0.308±0.082	0.307±0.083	0.351±0.094	0.350±0.096	0.245±0.044	0.244±0.044
R3	0.006±0.000	0.011±0.003	0.011±0.003	0.011±0.003	0.013±0.003	0.013±0.003	0.009±0.001	0.009±0.001

'ref' refers to mean amounts during reference period 1971-2000. 'fut' refers to mean amounts during future period 2070-2099. Values given are the mean ± standard deviation of the five climate models.

784

785 **Table 3: Proportion [%] of area dominated by climate or land use change impacts.**

	significantly changed fraction			*climate change dominated*[1]			*land use change dominated*[1]			*balanced*[1]		
	A1B	*A2*	*B1*	*A1B*	*A2*	*B1*	*A1B*	*A2*	*B1*	*A1B*	*A2*	*B1*
POC												
GOV	50.85	50.91	50.86	58.8	58.7	54.9	40.9	40.7	44.6	0.3	0.6	0.5
BAU	50.80	50.85	50.85	42.3	43.7	40.1	57.5	56.2	59.8	0.2	0.1	0.1
IC												
GOV	50.80	50.80	50.80	100.0	100.0	100.0	0.0	0.0	0.0	0.0	0.0	0.0
BAU	50.80	50.80	50.80	100.0	100.0	100.0	0.0	0.0	0.0	0.0	0.0	0.0
outgassed carbon												
GOV	97.6	97.60	97.61	70.5	77.7	68.4	29.3	22.3	31.1	0.2	0.0	0.4
BAU	97.55	97.65	97.60	52.4	56.9	50.2	47.6	43.0	49.7	0.1	0.1	0.1

786 If both impacts compensate each other the cell is balanced. [1]The proportions refer to the
787 significantly changed overall fraction (first columns).

8 Figures

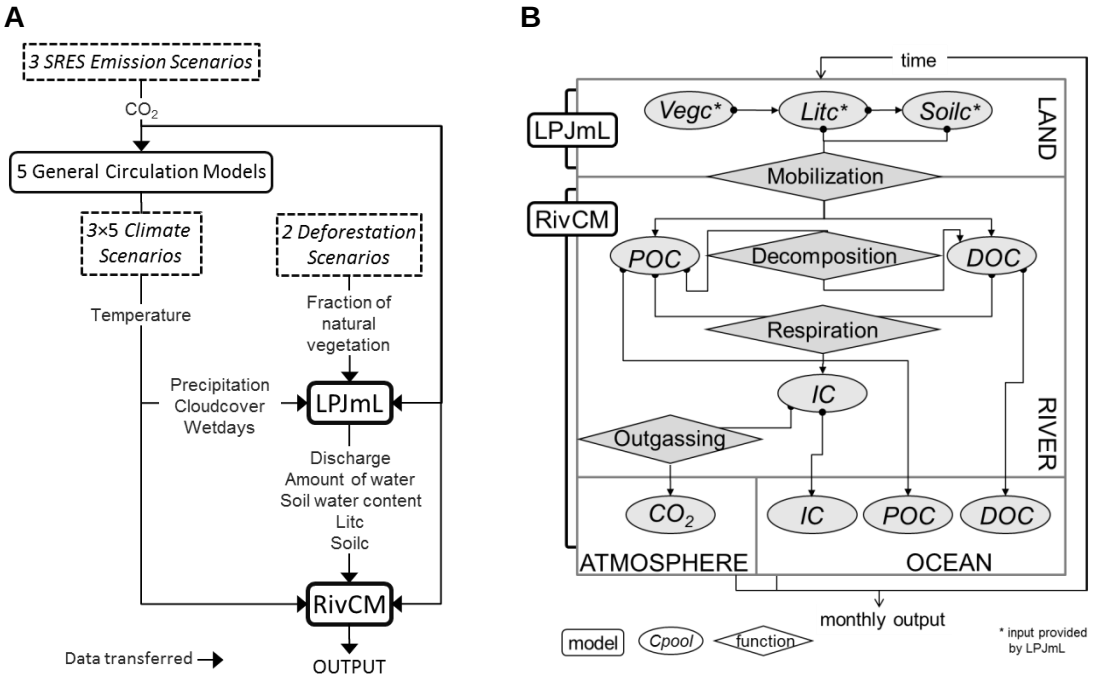

Figure 1: Overview of the general transfer of data between scenarios and models (A) and the detailed calculation of carbon fluxes within and between LPJmL and RivCM.

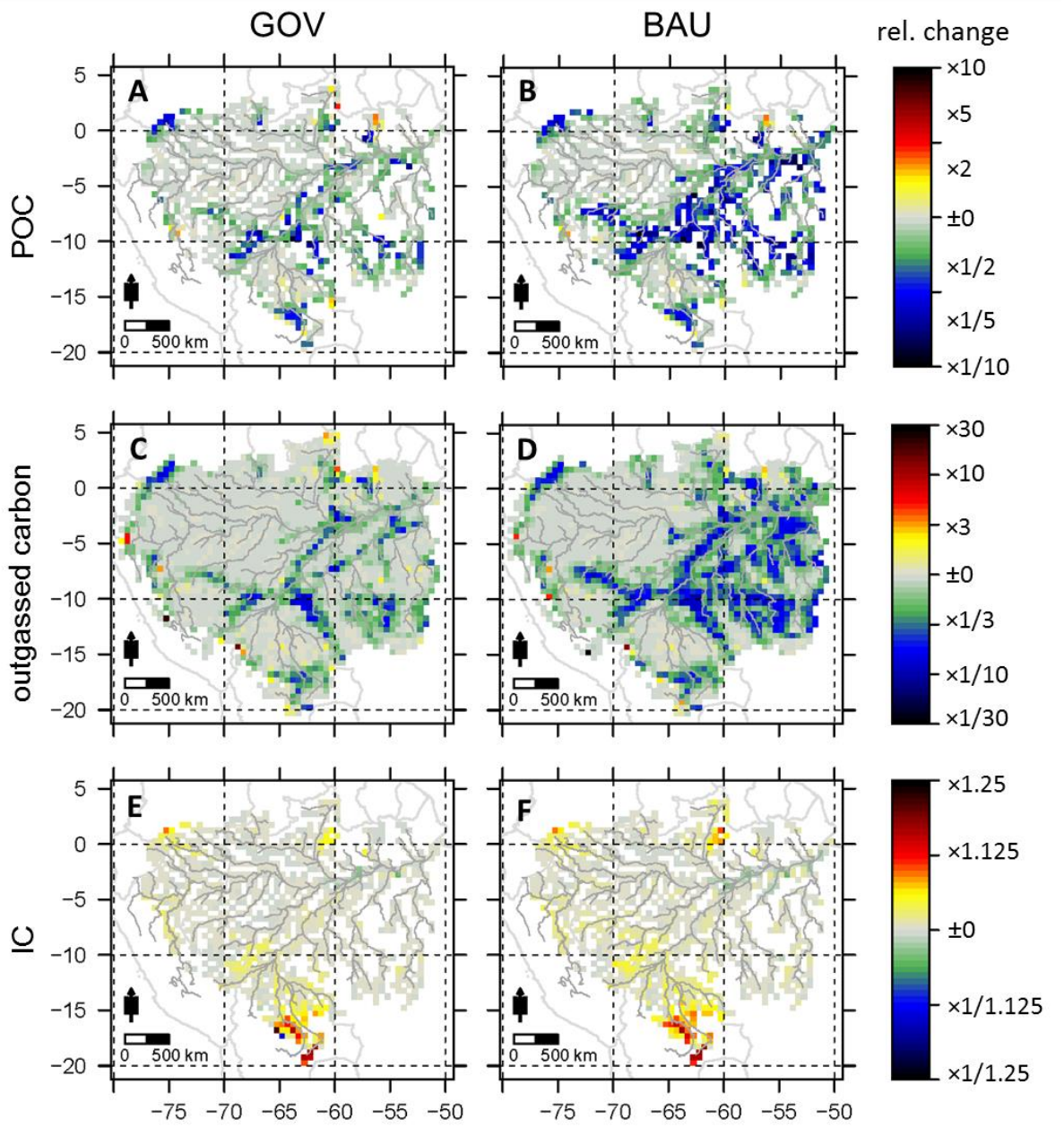

793

794 **Figure 2: Change in carbon caused by deforestation.** Climate model mean (E_{Defor}) of the
795 change of particulate organic carbon POC (A, B), outgassed carbon (C, D) and inorganic
796 carbon IC (E, F). Results of the SRES emission scenario A1B are averaged over five climate
797 models. Areas in yellow and red indicate a gain and areas in green and blue indicate a loss in
798 carbon caused by deforestation (GOV and BAU).

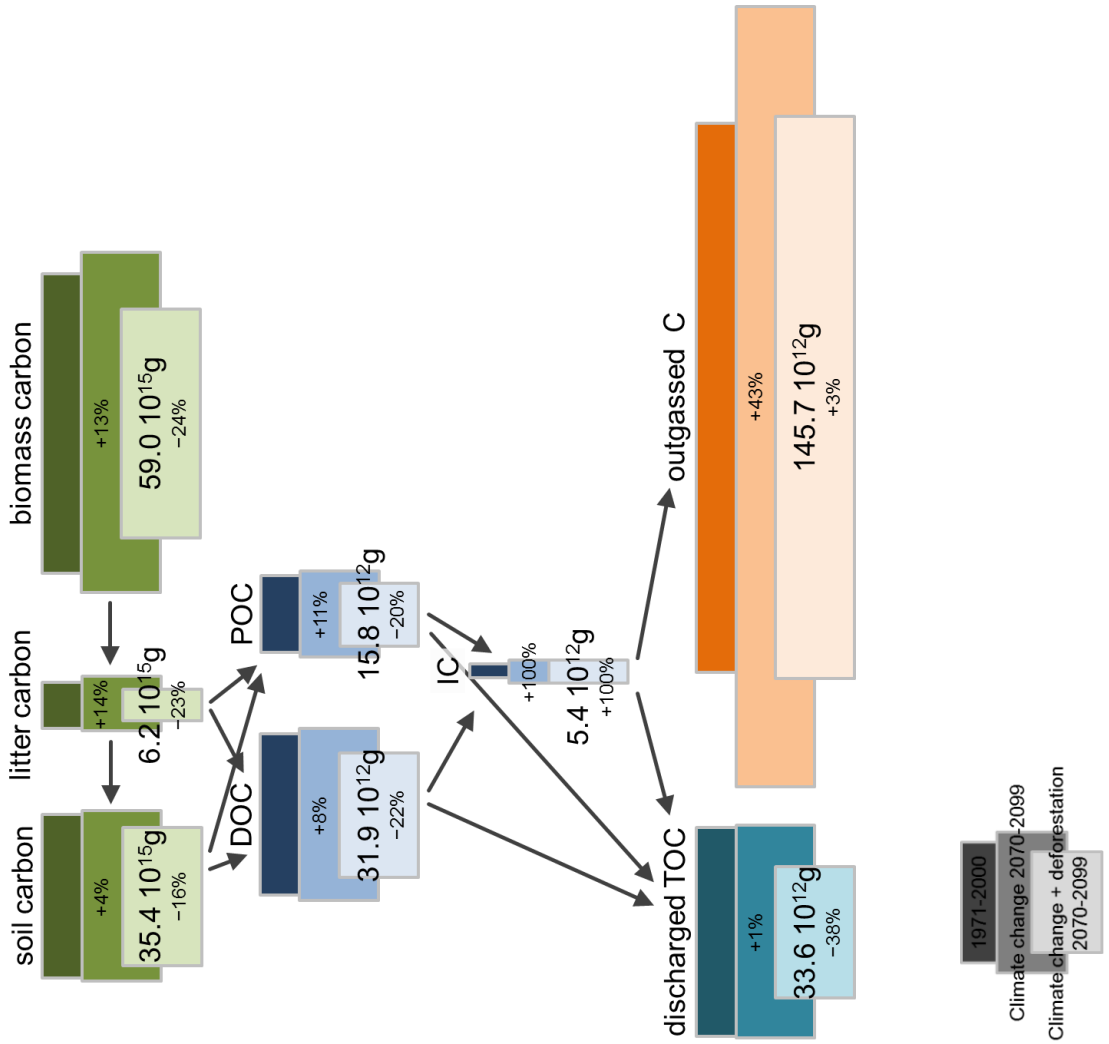

Figure 3: Averaged annual amounts and change in the basin carbon budget due to climate change and deforestation. Dark boxes indicate the amount of carbon during the reference period (1971-2000), intermediate boxes during the future period (2070-2099) under climate change only (Langerwisch et al., 2015), light boxes during the future period under the forcing of climate change and deforestation (BAU) together (average over all SRES scenarios and GCMs). Amount is given for future period with relative change compared to reference. Arrows indicate the direction of carbon transfer.

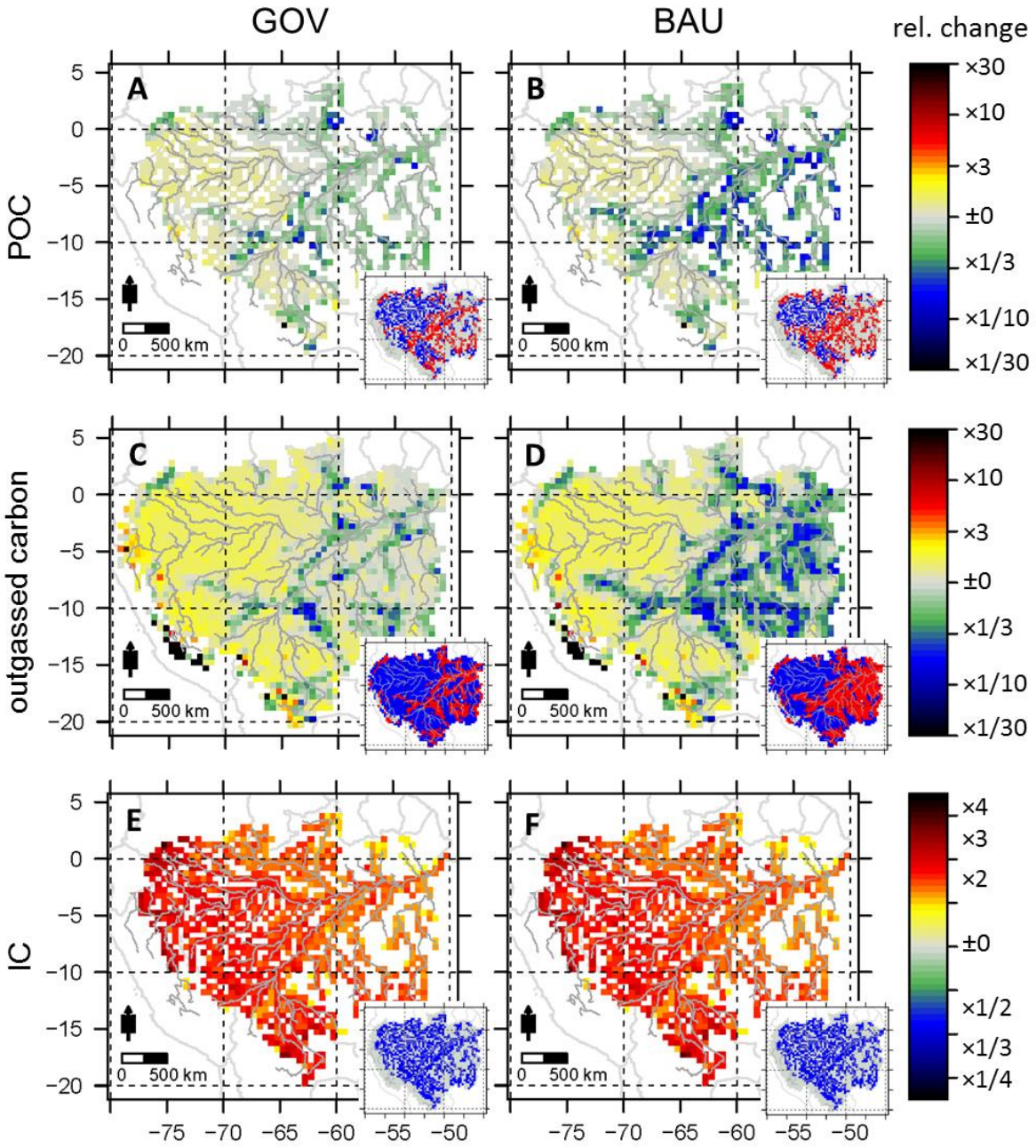

Figure 4: Change in carbon caused by deforestation and climate change. Climate model mean ($E_{CCDefor}$) of the change of particulate organic carbon POC (A, B), outgassed carbon (C, D) and inorganic carbon IC (E, F). The inset maps show blue areas where changes are predominantly caused by climate change and red areas where changes are predominantly caused by deforestation. For further details see Figure 2.

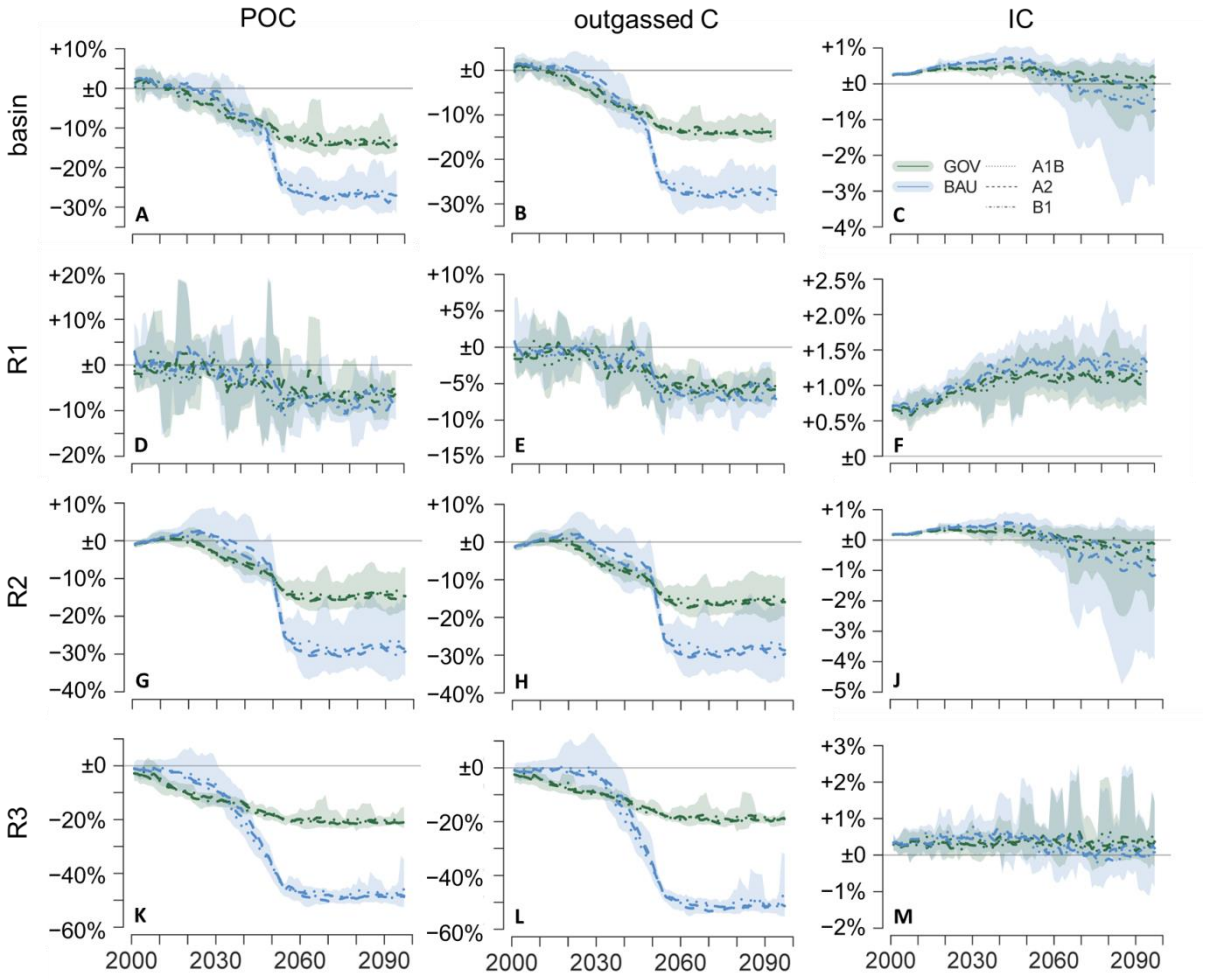

Figure 5: Temporal change in particulate organic carbon due to land use change. Change of annual sum of carbon in the deforestation scenario (GOV or BAU) compared to the NatVeg scenario (average over 1971-2000) for the whole basin (A-C) and the three sub-regions (R1-R3; D-M) as 5-year-mean for GOV (green) and BAU (blue). The shaded areas indicate the full range of values of all five climate models. Bold lines represent the 5-year-mean of the five climate models.

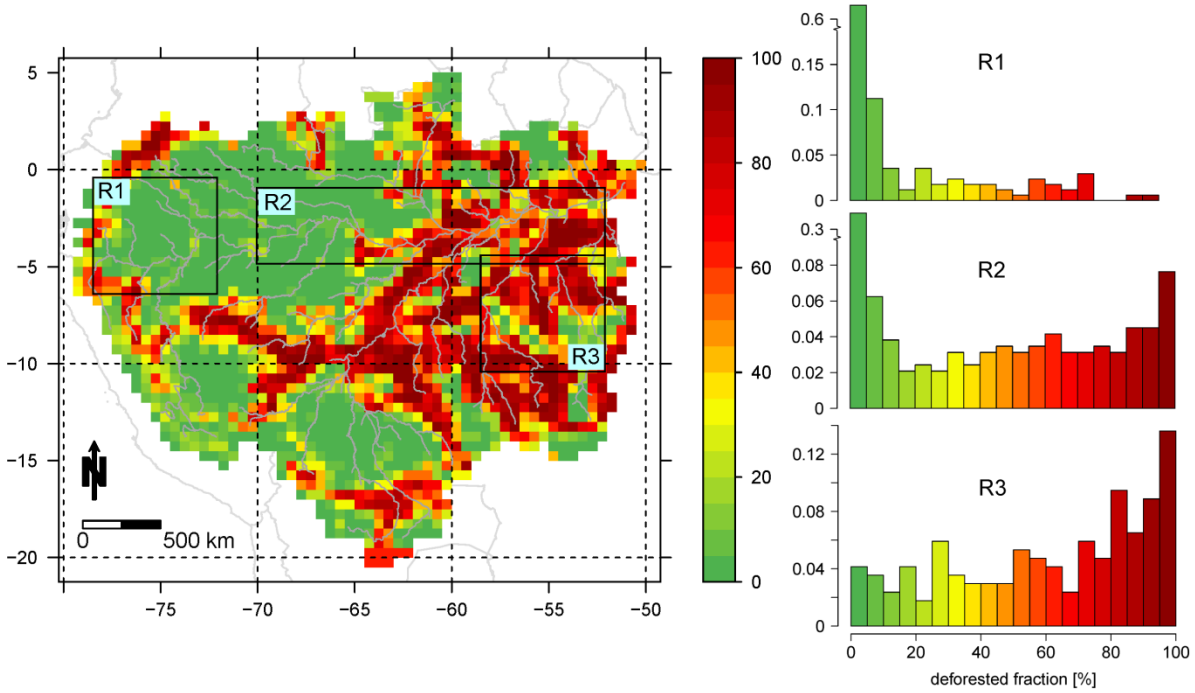

Figure S1: Fraction of deforested area per cell [%] in 2050. Data are based on Soares-Filho et al. (2006). The three sub-regions discussed in the main text are highlighted in the map. The histograms (right panels) show the proportion of 20 deforestation classes (0-5% deforested to 95-100% deforested) in each sub-region.

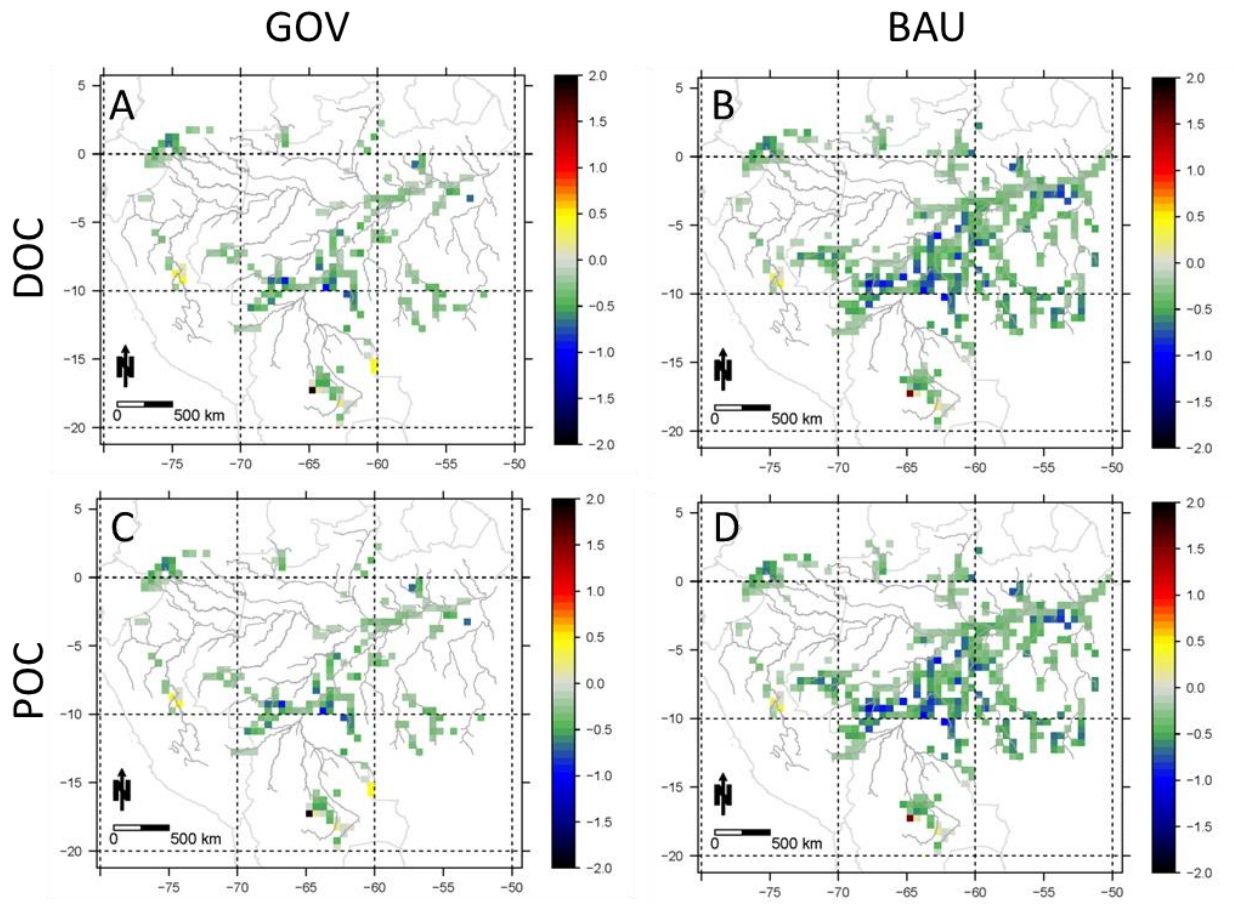

831

832 **Figure S2: Similar change in dissolved (A, B) and particulate organic carbon (C, D) due**
833 **to deforestation.** SRES scenario is A1B, climate model is MPI-ECHAM5. Positive values
834 (yellow and red) indicate a gain and negative values (green and blue) indicate a loss in carbon
835 caused by deforestation (GOV and BAU). Only cells with significant changes ($p<0.05$,
836 Wilcoxon Rank Sum Test) are shown.

837